Bei Li [1], Youtian Niu [1,2,3,4], Zhaodi Wang [1], Kangpo Zhou[1], Songhao Guo [1], Xiukun Zhao [1], Zhe Wang [1], Sai Yang[1], and Zhiyuan Zheng [5]

[1]College of Electronic and Electrical Engineering, Henan Normal University, Xinxiang, Henan, PR China

[2]Academician Workstation for Electromagnetic Wave Engineering in Henan Province, Xinxiang, Henan, PR China

[3]Key Laboratory of Integrated Application of Optoelectronic Sensing in Henan Province, Xinxiang, Henan, PR China

[4]Henan Provincial Engineering Laboratory of Additive Smart Manufacturing, Xinxiang, Henan, PR China

[5] School of Shipping and Ship Engineering, Chongqing Jiaotong University, Chongqing, PR China

Corresponding author: Y.T. Niu (niuyt22@163.com)

Key Points:

- No satellites are required to predict solar flare class using the very low frequency method
- An accurate formula for the path from Hainan to Alpha navigation system is fitted according to 103 groups of VLF signal phase variation data
- Geomagnetic storms and energetic particles can be predicted 1-3 days in advance after predicting the class of flares

Abstract

Solar flares are the most violent outbursts that occur in localized regions of the solar atmosphere. They emit large amounts of X-rays and energetic particles. X-rays reaching the earth at the speed of light will disrupt the calm ionospheric environment, causing sudden ionospheric disturbance (SID), which will make the very low frequency (VLF) signal to sudden phase anomaly (SPA), lead to the positioning error of satellite navigation system and interfere with satellite communication. Energetic particles will arrive near the satellite orbit in 1-3 days, causing direct damage to the satellite. They may also cause geomagnetic storms after reaching the Earth. In this paper, we mainly study to monitor solar activity and calculate solar flare class through the phase variation of VLF signal by combining the theory of VLF waveguide mode in order to forecast the environment of satellite navigation and communication. In addition, it can also predict the energetic particles and geomagnetic storms 1-3 days in advance according to the time and class of flare outbreak, so that the protective measures for satellite to operate safely could be taken in advance.

Plain Language Summary

The outbreak of solar flares has a huge impact on the ionosphere and the earth, which will make the satellite navigation system and satellite communication

system not work properly. In this paper, the class of solar flare is deduced by studying the effect of solar flare outburst on VLF signal phase. This provides real-time predictions of satellite navigation and communication environment, as well as predictions of energetic particles emitted by flares and possible geomagnetic storms 1-3 days in advance. The main advantage of VLF method is that it is cheaper, does not require any satellites, and the signal propagation is stable and will not be interrupted.

1 Introduction

The very low frequency refers to radio waves with frequency band of 3-30 kHz. It has low attenuation, long propagation distance, stable phase and strong ability to penetrate seawater, which propagates mainly in the earth-ionosphere waveguide (Yi et al., 2019). In recent years, with the development of science and technology, VLF has been widely used in many aspects such as submarine communication (Shi et al., 2011), prediction of earthquakes (Duan, 2020), detection of mineral resources (Bi, 2016), lightning localization (Niu et al., 2021) and monitoring of the near-Earth space environment (Cohen et al., 2009), etc.

The satellite navigation system consists of three parts: navigation satellites, ground stations and user positioning equipment (Yuan et al., 2003), which is an integrated satellite system achieving multi-purpose uses such as global high-precision navigation, geodesy and meteorological services. Satellite communication system is comprised of satellite terminal, ground terminal and user terminal. The satellite is equivalent to a relay station (Fu, 1980). Satellite communication belongs to microwave communication, which is an important means of international and domestic communication at present.

When the satellite signal passes through the ionosphere, its phase and frequency will be affected to some extent due to the irregular and uneven distribution of particles in the ionosphere, and phenomena such as Faraday rotation, Doppler effect, refraction, absorption, etc. will occur. The total electron content (TEC) of the ionosphere varies with time, geographical location and solar activity. The TEC varies regularly with time (sunrise and sunset, seasons, and 11-year solar activity cycle); However, sudden ionospheric disturbance events and ionospheric storms caused by solar activity are unpredictable. And satellites cannot be corrected for the ionospheric delay errors generated by such variations using space-based augmentation systems or differential systems, which may cause serious safety problems.

In the geomagnetically quiet state, the electrons in the ionospheric D-layer are mainly derived from direct radiation of Lyman- rays (Mitra, 1972) , extreme ultraviolet rays (Tsurutani et al., 2009) and direct radiation of cosmic rays (Selvakumaran et al., 2015) . When solar flares erupt, the sun will radiate a large number of X-rays, which will suddenly increase the ionization of the ionosphere D-layer (Huang et al., 2013), affecting the signal transmission between satellites and the earth's ground, resulting in the decrease of satellite navigation system accuracy(Berdermann et al., 2018), the decrease of signal-to-noise ratio and the

increase of bit error rate of satellite communication signals; in serious cases, it may even lead to the failure of navigation receivers and the interruption of satellite communication links (Zhou, 2017; Wu, 2014). In addition, when the energetic particles radiated from the sun reach the orbit of the satellite, they are likely to hit the important parts of the satellite, causing abnormal satellite operation or even satellite failure (Niu et al., 2013); if a solar flare happens to break out during the sun outage phenomenon, it will be more harmful to the satellite.

There are various methods to monitor solar activity and ionospheric environment around the globe: in 2006, the US launched the solar observation satellite STEREO that can display panoramic 3D images of solar activity to help scientists monitor the sun and study the impact of solar activity; Li et al. (2012) proposed the use of global positioning system (GPS) data monitoring of the land state network to carry out ionospheric space weather monitoring by analyzing the spatial and temporal characteristics of the total electron content of the ionosphere over China. In addition, there is also a method to measure ionospheric electron density by vertical sounding (Chen et al., 2021), then to monitor solar activity further. In contrast, China currently has fewer satellites for space weather forecasting, so there is still a large gap compared with foreign countries. Meanwhile, the use of satellites and GPS monitoring is not only expensive, but also requires processing a large amount of data, which is a complicated process (Niu et al., 2017).

By comparison, the VLF method studied in this paper has lower cost. Besides, as the VLF signal is very sensitive to SID events, the effective reflection height of the VLF signal decreases rapidly when SID events occur (Thomson & Clilverd , 2001), and sudden phase anomaly will occur (Su et al., 2018), the solar activity and ionospheric space environment can be known by simply observing its phase, so the method is sensitive, simple and intuitive. Compared with the vertical detection using short wave method, VLF has longer propagation distance, less limitations, stable signal propagation, and will not be interrupted by the bursts of solar flares.

2 VLF signal transmitting and receiving system

According to the waveguide mode theory, the ground and the lower edge of the low ionosphere are regarded as the two walls of the spherical shell waveguide, which constitutes the ground-lower-ionosphere waveguide. In the frequency band of VLF, except for a small portion of low-band electromagnetic waves, the rest of the frequency band is confined to propagate in the ground-lower-ionosphere waveguide, so its propagation effect is affected by the ionospheric D-layer in addition to the earth's surface (Thomson & Clilverd, 2001). The D-layer disappears at night, and the effect of solar flares on the phase of the VLF signal cannot be observed if both the VLF signal transmitter and receiver stations are in the evenings. However, the distance between the transmitting stations and receiving stations of the VLF signal used in this paper is relatively far, so the propagation path may be partly sunny and partly cloudy. The signal

response can be observed as long as there is a sunny side in the propagation path (Gu et al., 2021), so the daily observation and recording time would be longer.

To verify the feasibility of the method, the data received from two VLF signal receiving stations, located in Xinxiang, Henan, China and Hainan, China, were used in this paper. The VLF signal transmitting station is the Alpha navigation station located in Russia. The Alpha navigation system consists of the west sub-station in Krasnodar, the main Station in Novosibirsk, and the east sub-station in Khabarovsk, transmitting VLF signals at 11.9 kHz, 12.6 kHz, and 14.9 kHz. In this paper, the VLF signals of the main station to Xinxiang path and main station to Hainan path are analyzed, and the distances from the main station of the Alpha system to the receiving stations of in Xinxiang and Hainan can be calculated according to the great circle distance formula, which are about 3187.7km and 4546.7km respectively, and both of them are long-distance propagation. The receiving station can receive the VLF signals from the Alpha navigation system transmission 24 hours a day. The block diagram of the receiving system is shown in Figure 1. The VLF signal received by the antenna is sampled after passing through the low noise amplifier, anti-aliasing filter and automatic gain control. The standard sampling interval of the sampling pulse circuit used is provided by the rubidium atomic frequency standard. After sampling, conduct A/D conversion and input to the computer. The computer will feed back to the automatic gain control link according to the received signal, and accurately regulate the signal to ensure its accuracy.

Figure 1. Block diagram of the VLF signal's phase monitoring system

3 Theoretical and data analysis

The propagation of VLF between the earth-lower-ionosphere waveguides is less affected by ionospheric perturbations and is more stable. When the solar flare erupts, the SID event caused by it will reduce the effective reflection height of the ionosphere to the VLF signal, resulting in the sudden phase anomaly of the VLF signal, but it will not cause the signal interruption.

According to the "waveguide mode" theory (Wait, 1959; Liu, 1987), it is known that the phase velocity of the VLF signal when the ionosphere is in the calm state ν_p(m s^{-1}) can be expressed as:

$$\nu_p \approx v_c \left(1 - 0.36\frac{h_0}{a} + \frac{\nu_c^2}{32f^2h_0^2}\right) \quad (1)$$

Where ν_c is the speed of light in free space, which is about 2.998 $\times$ 10^8 m/s, and h_0 is the effective reflection height of the low ionosphere, and f is the VLF signal frequency, a is the average radius of the earth, which is about 6371.4 km.

The VLF phase variation Δ can be expressed as:

$$\Delta = \mathbb{d}\left(\frac{1}{v_p'} - \frac{1}{v_p}\right) \quad (2)$$

where $v_p^{'}$(m s^{-1}) is the phase velocity of the VLF signal when a solar flare bursts, and d is the great circle distance between the transmitter and the receiver.

Based on the above two expressions, the expression of $v_p^{'}$ can be obtained:

$$v_p^{'} = \frac{d \times v_p}{\Delta \times v_p + d} \quad (3)$$

Assume that the ionospheric effective reflectance height variation when the flare burst is h, the VLF signal phase radian change is $\varphi^{'} = 2\pi f \bullet \varphi$. The relationship between h and $\varphi^{'}$ can be expressed as:

$$h = \frac{h_0 \lambda}{2\pi \times d[0.36\frac{h_0}{a} + (\frac{\lambda}{4h_0})^2]} \times \varphi^{'} \quad (4)$$

This leads to the relationship between φ and h:

$$h = \frac{h_0 v_c}{d[0.36\frac{h_0}{a} + (\frac{v_c}{4h_0 f})^2]} \times \varphi \quad (5)$$

On the path from Xinxiang to the main station, the fitting equation of the relationship between the peak flux density of X-ray and the ionospheric effective reflectance height variation is (Zhang, 2014):

$$F_0 = 3.633e^{0.7476|\Delta h|} \times 10^{-3} \quad (6)$$

Because of the different observation paths in Hainan, the relationship between the peak flux density of X-ray and the variation of the ionospheric effective reflectance height are re-fitted in this paper. Based on the 103 flare phase anomalies observed by the VLF receiver from 10:00 to 17:00 in 1999 and 2000, the path from Hainan to the main station was fitted with the least square method, and the fitted equation was obtained as:

$$F_0 = 2.1053e^{0.3574|\Delta h|} \times 10^{-3} \quad (7)$$

The class of a solar flare can be predicted by calculating the peak flux density of X-ray according to Equations (6) and (7) respectively.

From a news report from the Central Meteorological Administration (CMA, 2003), in May 1998, a solar flare caused a complete failure of the U.S. Galaxy 4 satellite, paralyzing 80% of pagers and radios in North America, throwing financial services into chaos and forcing credit card transactions to be interrupted; and causing a 6-hour data loss on the Polar spacecraft.

In Xinxiang, Henan province, we have plotted the change curve of amplitude and phase of VLF signal by receiving VLF signal of three frequencies from the main station of Russian Alpha navigation station. The VLF signal change curve on 6 May 1998 is shown in Figure 2. The red, blue and green curves in the figure represent VLF signals with frequencies of 11.9kHz, 12.6kHz and 14.9kHz respectively. Normally, the Phase curve should be stable. When the curve is raised, a sudden phase anomaly occurs, indicating that a solar flare may burst at this time. In this paper, the phase change φ caused by SPA phenomenon of VLF signals at three frequencies of the main station was calculated. The class of solar

flare was predicted according to the curve and formula, and its average value was calculated. This results are shown in Table 1. Where $\Delta\varphi_1$ $\Delta\varphi_2$ and $\Delta\varphi_3$ represent the phase changes of three VLF signals with frequencies of 11.9kHz, 12.6kHz and 14.9kHz respectively. In addition, the solar flare data released by GOES satellite is listed in Table 2(https://satdat.ngdc.noaa.gov/sem/goes/data/full/), and this data is compared with its according calculated results. In the table, "Start" is the start time of solar flare, "Max" is the peak time, "End" is the end time, "LT" stands for local time, "UT" stands for universal time, "X-ray" represents the solar flare class corresponding to the X-ray emitted during solar flare eruption, "Region" represents the serial number of flare eruption region on the sun. "Flux" indicates the flux released during the flare eruption process, and its unit is W m^{-2}. The observed data in this paper are based on local time records, but the data recorded by the GOES satellite in the United States is based on universal time, the relationship between the local time LT used in this paper and universal time UT is LT=UT+8.

Figure 2. VLF signal phase versus time curve of different frequencies on 6 May 1998 under the path from Alpha main station to Xinxiang

Table 1

Solar Flare Data of 6 May 1998 Monitored by VLF Signal Phase Monitoring System under the Path from Alpha Main Station to Xinxiang

	Start	Max	End	Main station VLF signal anomaly	Flare pre
Date	(LT)	(LT)	(LT)	11.9kHz	12.6kHz
				$\Delta\varphi_1(cec)$	$\Delta\varphi_2(cec)$
06	0727	0746	0727	11.85	11.97
	1253	1306	1317	5.83	6.47
	1510	1525	1541	14.20	12.89
	1558	1609	1620	23.54	22.01

Table 2

Solar Flare Monitored by the GOES

	Start	Max	End	NOAA/USAF		
Date	(UT)	(UT)	(UT)	Xray	Region	Flux
05	2327	2346	0002	M2.5	8210	3.4E-02
06	0453	0506	0517	C8.4		8.9E-03
	0710	0725	0741	M2.9	8210	3.7E-02
	0758	0809	0820	X2.7		2.1E-01

By comparing the final results of the calculation with the data monitored by the GOES satellite, we found that it is possible to monitor flares by the VLF

phase variation, and to roughly calculate the class of solar flares, which in turn leads to the state of the ionosphere and the immediate environment for satellite navigation and communication.

In addition to this solar storm, in late October and early November 2003, during the Halloween season in Western countries, the sun erupted in the strongest flare ever observed by the GOES, known as the "Halloween Storm". As a result of this storm, GOES, ACE, SOHO, WIND and other important scientific research satellites in Europe and the United States were damaged to varying degrees, and the Japanese Echo satellite went out of control; the Kodama satellite went into safe mode and did not resume normal operation until 7 November; the Chandra and SIRTF satellites were interrupted. interrupted; Polar satellite TIDE instrument automatically restarted, high-voltage power supply was damaged, 24 hours later to restore normal; NASA's Mars exploration satellite Odyssey spacecraft MARIE observation equipment was completely destroyed by particle radiation, the incident also caused the Shenzhou V spacecraft to significantly lower the altitude of the orbital module, so measures had to be taken to raise the orbit of the spacecraft to avoid an early crash (CMA, 2013). In addition, the GPS was also affected, with deviations in positioning accuracy, which also paralyzed flights and other transportation systems requiring instant communication and positioning to varying degrees, causing great losses.

We chose 26 October to 4 November 2003 to observe this solar flare in Hainan, China, and plotted the VLF signal variation curves for 31 October and 3 November, as shown in (a) and (b) in Figure 3 respectively.

Figure 3. (a) VLF signal phase versus time curve of different frequencies on 31 October 2003 under the path from Alpha main station to Hainan, (b) VLF signal phase versus time curve of different frequencies on 3 November 2003 under the path from Alpha main station to Hainan

The data derived and predicted from the VLF signal variations are shown in Table 3; the solar flare data recorded by the US GOES satellite are shown in Table 4.

Table 3

Solar Flare Data Monitored by VLF Signal Phase Monitoring System under the Path from Alpha Main Station to Hainan

	Start	Max	End	Main station VLF signal anomaly	Flare pred
Date	(LT)	(LT)	(LT)	11.9kHz $\Delta\varphi(cec)$	12.6kHz $\Delta\varphi(cec)$
10.31	1226	1233	1237	15.91	15.71
	1408	1416	1428	9.12	8.46
11.03	0909	0930	0945	30.62	30.18
	1743	1755	1819	37.51	32.25

Table 4

Solar Flare Monitored by the GOES

Date	Start (UT)	Max (UT)	End (UT)	NOAA/USAF Xray	Region	Flux
31 October	0426	0433	0437	M2.0		9.2E-02
	0608	0616	0628	M1.1	10488	1.1E-02
3 November	0109	0130	0145	X2.7	10488	3.6E-01
	0943	0955	1019	X3.9	10488	5.6E-01

With the burst of solar flares, in addition to the X-rays that reach the earth in about 8.3 minutes and affect the satellite navigation and communication environment, a large amount of energetic particles radiated from the sun will reach the earth in about 1-3 days later. The energetic particles can cause direct damage to satellites: the radiation dose effect can cause radiation damage to the materials, components, and solar cells of satellites; energetic particles can also lead to single-particle effects in satellites, which can cause confusion in satellite operation program and produce spurious instructions; the charge-discharge effect can cause static electricity on the surface and inside of satellites, and the electrostatic discharge can damage devices or materials, and in serious cases, permanently destroy them. Moreover, it is highly likely that energetic particles will cause geomagnetic storms after reaching the earth. During geomagnetic storms, the current in the ionosphere and the energetic particles deposited into the ionosphere increase energy in the form of heat, which increases the density and density distribution in the upper atmosphere, causing additional drag on satellites in low Earth orbit, resulting in a decrease in satellite orbital altitude, a decrease in lifetime, and eventually an early fall. In addition to this, local heating also produces strong horizontal changes in the ionospheric density, which can alter the path of radio signals and create perturbations in the signals, affecting satellite communication and GPS positioning navigation (Mcknight & Darren., 2017; Liu, 2016; Iucci et al., 2006; Afraimovich et al., 2009; Demyanov et al., 2021).

Table 5 lists some flares with magnitude greater than M-class observed by GOES from 26 October 2003 to 3 November 2003, compared with the data predicted in this paper based on the amount of phase change of the VLF signal, some of which are not recorded due to equipment maintenance.

Table 5

Comparison of VLF Signal Phase Monitoring System with GOES Recorded Data

Date	Start (UT)	Max (UT)	End (UT)	NOAA/USAF Xray	Flare prediction class	Region	
26 October	0557	0654	0733	X1.2		10486	-

28 October	0951	1110	1124	X17.2	10486	-
29 October	0026	0151	0208	M1.1	10486	M1.4
	0408	0511	0554	M3.5		M5.0
30 October	0156	0207	0229	M1.6	10488	M1.2
31 October	0426	0433	0437	M2.0		M2.4
	0608	0616	0628	M1.1	10488	C8.0
03 November	0109	0130	0145	X2.7	10488	X2.2
	0943	0955	1019	X3.9	10488	X4.0

It can be seen from the data in the table that during this period, solar activity was intense, and a large number of M- and X-class flares burst in a short time. A large number of energetic particles would reach the earth in about 1-3 days, and it was very likely to cause geomagnetic storms. According to the time of flare burst and the calculated flare class, we speculate that the solar flare occurred on 26 October may cause energetic particle deposition event and geomagnetic storms from 27 October to 29 October. Later, the X-class flare that burst on 28 October may have kept the flow of energetic particle flux at a high level, causing geomagnetic storms to persist; Following the continuous eruption of five flares on 29 October, 30 October and 31 October, we speculate that the energetic particles emitted by them will reach the earth from 30 October to 4 November, and may continue to rise after a slow decrease in the flux of energetic particles. Finally, energetic particles emitted from the 3 November X-class flare could reach the earth's vicinity between 4 November and 6 November, triggering geomagnetic storm again.

Partial data of the energetic particle flux monitored by GOES from 28 October to 5 November 2003, are shown in Figure 4. It can be seen from the data that the energetic particle flux increased at UT12:00 on 28 October, which may be caused by the X-class flare on 26 October. There were continuous flares on 28 October. It can be seen that the upward trend of the energetic particle flux continued until UT10:00 on 29 October and then began to decrease slowly. However, it is a pity that the phase changes of VLF were not recorded due to equipment overhaul. Then, the energetic particle flux repeatedly increased and decreased on 30 November, which was presumed to be caused by two M-class flares on 29 November. After that, the flux of energetic particle flux decreased slowly from 31 October, and then increased sharply at UT18:00 on 2 November, which was speculated to be caused by the continuous eruption of two M-class flares on 31 October. Then we can see that the energetic particle flux decreased slowly on 4 November, but there was an insignificant upward trend at UT10:00 on that day, which was inferred to be caused by the X2.7 solar flare on 3 November. However, as the energetic particle flux kept at a high level, there was no obvious upward trend. After a slow decline, what can be known is that the energetic particle flux starts to rise again at UT23:00 on 4 November, which is presumed to be caused by the X3.9 class flare on 3 November. It was not until about UT05.00 on 5 November that the energetic particle flux showed a slow downward trend

and tended to be stable all the time. This series of records is basically in line with our predictions.

Figure 4. Energetic particle flux observed by GOES

The following figure lists the Kp index and Dst index in October and November 2003 from the GOES. The K index is a "3-hour magnetic index" that measures the intensity of geomagnetic disturbances at a single geomagnetic station over a 3-hour period. The level from 0-9 indicates that the amplitude of geomagnetic disturbance increases gradually. The Kp index is calculated from the K index from 13 geomagnetic stations in the global geomagnetic network. By comparing the intensity of geomagnetic disturbance shown by Kp index with the predicted time of geomagnetic storm, it is found that the two are relatively consistent. There were indeed strong geomagnetic storms with Kp=9 from 29 October to 30 October, which lasted longer. Small and medium geomagnetic storms also occurred on 4 November. Dst is a geomagnetic index used at low- and mid-latitude test stations to measure changes in the intensity of the horizontal component of the geomagnetic field. A smaller Dst indicates a gradual increase in the magnitude of the magnetic disturbance. A small geomagnetic storm is considered to occur when -50nT Dst < -30nT; a medium geomagnetic storm is considered to occur when -100nT Dst < -50nT; and a strong geomagnetic storm is considered to occur when Dst -100nT (Xie et al. 2004). From the Dst index records released by GOES, we can see that the Dst index decreased below -100nT at 08:00 UT on 29 October sharply, and reached negative extremes frequently on the 29-31 October, where the minimum value even reached -401nT; moreover, the Dst index remained at a level less than - 30nT between 1 November and 6 November, indicating that the medium and small geomagnetic storms persisted after the strong geomagnetic storms' ending. This series of geomagnetic storms resulted in the malfunction of GPS and LORAN navigation systems, multiple satellites' losing contact with the ground for several hours. Besides, the global navigation system was also affected, having problems in positioning accuracy. (Wang, 2017)

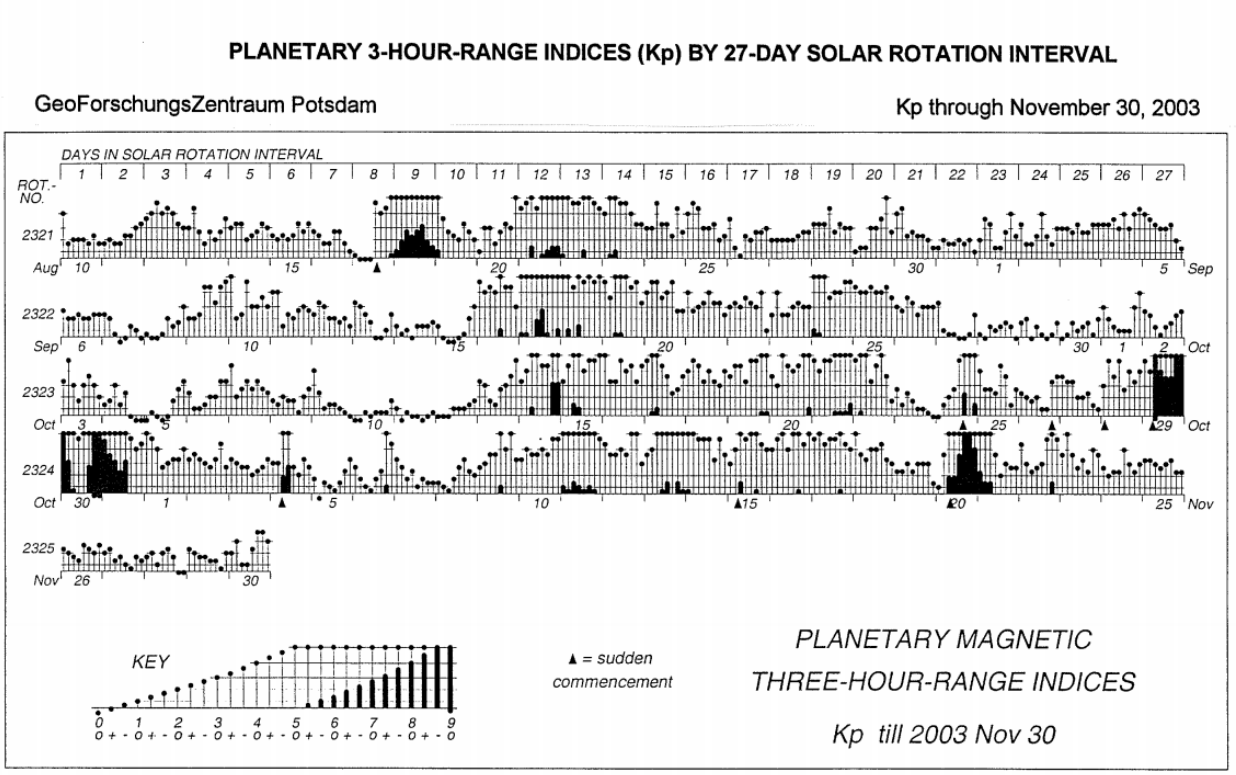

5. Kp index records from August to November 2003

Figure 6. (a) Dst index records for October 2003, (b) Dst index records for November 2003

There have been numerous incidents where geomagnetic storms have caused significant harm to satellites. In a recent news report, we learned that the latest batch of 49 Starlink satellites deployed by SpaceX have been hit by geomagnetic storms and up to 40 satellites are about to crash or have crashed into the atmosphere and be destroyed. According to the data, the satellites encountered a Kp=5 geomagnetic storm the day after launch, increasing their operational drag by 50%. Although the team directed the satellites into "safe mode" and tried to change their attitude to reduce drag, the increased drag prevented 40 satellites from exiting safe mode to lift their orbits and had to re-enter the atmosphere to be destroyed (Ou, 2022). From these events, it is clear that advance prediction of geomagnetic storms is essential for satellites.

4 Summary and Discussion

Solar flares not only affect the earth's ionosphere, but also cause serious impacts on the satellite navigation and communication environment, such as interruption of satellite communication links and serious degradation of navigation accuracy.

In this paper, we analyze the phase change of VLF signal in 1998 and 2003, and combine the phase change of VLF with waveguide mode theory to monitor the ionospheric environment and solar flares, and calculate the solar flare class to forecast the satellite navigation and communication environment. In addition, after calculating the solar flare class, it is possible to predict the arrival of energetic particles and the geomagnetic storms triggered by them in 1-3 days, so that defensive measures can be taken in advance to ensure the safety of satellites and to ensure the reliability of satellite communication and navigation. Unfortunately, the VLF method cannot be observed due to equipment maintenance or the occurrence of flares at night, and the prediction results still have some errors with the real data, so we need to continue to fit a more accurate formula by observing a large amount of data in the future.

Acknowledgements

This study has been supported by the National Natural Science Foundation of China (U1704134) and Henan Provincial Key Scientific and Technological Research Projects (162102210263, 172102310238).

Open Research

The X-ray dates used in this paper are from the National Oceanic and Atmospheric Administration (NOAA) website: https://satdat.ngdc.noaa.gov/sem/goes/data/full/. The local data in this paper were observed and collected by Professor You-tian Niu when he was working at the China Institute of Radio Wave Propagation.

References

Afraimovich, E. L., Astafyeva, E. I., Demyanov, V. V., & Gamayunov, I. F. (2009). Mid-latitude amplitude scintillation of GPS signals and GPS performance slips. *Advances in Space Research, 43*(6),964-972. http://doi.org/10.1016/j.asr.2008.09.015

Berdermann, J., Kriegel, M., Banyś, D., Heymann, F., Hoque, M. M., & Wilken, V., et al. (2018). Ionospheric response to the X9.3 Flare on 6 September 2017 and its implication for navigation services over Europe. *Space Weather, 16*(10), 1604–1615. https://doi.org/10.1029/2018SW001933

Bi, Y. X. (2016). Research on Metal Prospecting VLF Method Based on Software Radio. (Master's thesis). Retrieved from CNKI. (https://kns.cnki.net/kcms/detail/detail.aspx?dbcode=CMFD&dbname=CMFD201701&filename=1016234464.nh&uniplatform=NZKPT&v=z_6A7iLT62EuWKfwXY71XB6ZgscM-RUHGj3mu4gEq5VMh0_P2QO8J2o4o6h547V). Xinxiang, China: *Henan Normal University*.

Chakrabarti, S. K., Sasmal, S., & Chakrabarti, S. (2010). Ionospheric anomaly due to seismic activities - Part 2: Evidence from D-layer preparation and disappearance times. *Natural Hazards and Earth System ciences, 10*(8), 1751-1757. https://doi.org/10.5194/nhess-10-1751-2010

Chen, Y. L., Fu, W., Zhao, Y. L., & Han, J. (2021). Ionospheric sounding and prediction of ionospheric disturbance. *China Radio,* (01), 40-42.

CMA. (2013). *Impact of space weather disasters*. Beijing, China: China Meteorological News Service. http://2011.cma.gov.cn/ztbd/20110104/20110817/2011081710/201108/t20110818_101833.html

Cohen, M. B., Inan, U. S., & Paschal, E. W. (2009). Sensitive broadband ELF/VLF radio reception with the AWESOME instrument. *IEEE Transactions on Geoscience & Remote Sensing, 48*(1), 3-17. https://doi.org/10.1109/TGRS.2009.2028334

Demyanov, V. V., & Yasyukevich, Yu V. (2021). Space weather: risk factors for global navigation satellite systems. *Solnechno-Zemnaya Fizika, 7*(2),30-52. http://doi.org/10.12737/szf-72202104

Duan, Q. (2020). Research on the model of very low frequency signal propagation for earthquake prediction. (Master's thesis). Retrieved from CNKI. (https://kns.cnki.net/kcms/detail/detail.aspx?dbcode=CMFD&dbname=CMFD202102&filename=1020659414.nh&uniplatform=NZKPT&v=m4EmTqRipSiSrI2L0Pgwa10YivsSThzqW6mAoVHRo3j5Rqqx0DxyriO6___v3hg6w). Xinxiang, China: *Henan Normal University.*

Fu. D. D. (1980). The influence of satellite communication on human society. *Space International*, (01), 1-5+9.

Gu, X. D., Luo, F., Peng, R., Li, G. J., Chen, H. & Wang, S. W., et al. (2021). Response characteristics of very low frequency signals from JJI transmitter to solar flare events. *Chinese Journal of Geophysics*, *64*(5), 1508-1517.

Huang, J., Lin, G. G., Deng, B. C., Xu, J., & Kong, D. B. (2013). The study of solar flares effect on ionosonde data. *North China Earthquake Science*, *31*(04), 22-26+59. http://doi.org/10.3969/j.issn.1003-1375.2013.04.005

Iucci, N., Dorman, L. I., Levitin, A. E., Belov, A. V., Eroshenko, E. A., & Ptitsyna, N. G., et al. (2006). Spacecraft operational anomalies and space weather impact hazards. *Moon and near-Earth Objects, 37*(1), 184-190. http://doi.org/10.1016/j.asr.2005.03.028

Li, Q., Ning, B. Q., Zhao, B. Q., Ding, F., Zhang, R., & Shi, H. B., et al. (2012). Applications of the CMONOC based on GNSS data in monitoring and investigation of ionospheric space weather. *Chinese Journal of Geophysics, 55*(07), 2193-2202.

Liu, P. C. (2016). Research on the Effects that Solar Activity has on the Single Event for Space Instrument. (Master's thesis). Retrieved from CNKI. (https://kns.cnki.net/kcms/detail/detail.aspx?dbcode=CMFD&dbname=CMFD201901&filename=1018997653.nh&uniplatform=NZKPT&v=hgdzfaS-yTK6jmpGkoyOFD2DZwx_xo6R--2qxC5PhhWqsq2lqiSUIRsWoUwGkWd). Hunan, China: *National University of Defense Technology.*

Liu, W. T. (1987). Analysis of the correlation between sudden VLF phase anomalies and solar X-ray events. *Journal of Space Science, 007*(003), 185-189.

Mcknight & Darren. (2017). Examination of spacecraft anomalies provides insight into complex space environmentt. *Acta Astronautica, 158*(MAY), 172-177. http://doi.org/10.1016/j.actaastro.2017.10.036

Mitra, A. P. (1972). Interpretation of Ionospheric Effects of Solar Flares. Dordrecht: Astrophysics and Space Science Library.

Niu, Y. T., Piao, J. L., Su, Y. F., & Zhang, Y. M. (2017). Analysis of particle sedimentation and solar flares on VLF propagation in mid-latitude region. *Journal of Henan Normal University (Natural Science Edition), 45*(6), 31-36. http://doi.org/10.16366/j.cnki.1000-2367.2017.06.005

Niu, Y. T., Wang, L., Li, W. Q. (2021). Lightning VLF location based on waveguide mode theory and drosophila algorithm. *Insulators and Surge Arresters,* (01), 9-15. http://doi.org/10.16188/j.isa.1003-8337.2021.01.002

Niu, Y. T., Zhang, T. X., Xie, Y. T., Li, L., & Li, D. D. (2013). Forecast on solar flare during the launch of "Shenzhou " with the VLF method. *Science Technology and Engineering, 13*(35), 10575-10578.

Ou, S. (2022). U.S. *"Starlink" loses up to 40 satellites in geomagnetic storm.* (008). Beijing, China: Xinhua Daily Telegraph. http://doi.org/10.28870/n.cnki.nxhmr.2022.001103

Selvakumaran, R., Maurya, A. K., Gokani, S. A., Sneha, A., Veenadhari, B., & Kumar, et al. (2015). Solar flares induced D-region ionospheric and geomagnetic perturbations. *Journal of Atmospheric and Solar-Terrestrial Physics, 123*, 102-112. http://doi.org/10.1016/j.jastp.2014.12.009

Shi, W., Nao, X. F., & Hu, D. M. (2011). Ultra low frequency radio communication technology and its application in foreign submarine communication. *Digital Technology Applications,* (07), 12-13+15. http://doi.org/10.19695/j.cnki.cn12-1369.2011.07.010

Su, Y. F., Zhang, Y. X., Niu, Y. T., Piao, J. L., Wang, C. F., & Dong, L. Y. (2018). Continuous solar flares the effects analysis on the VLF signal propagation. *Progress in Geophysics, 33*(3), 969-972. http://doi.org/10.6038/pg2018BB0230

Thomson, N. R., & Clilverd, M. A. (2001). Solar flare induced ionospheric D-region enhancements from VLF amplitude observations. *Journal of Atmospheric & Solar Terrestrial Physics, 63*(16), 1729-1737. https://doi.org/10.1016/S1364-6826(01)00048-7

Tsurutani, B. T., Verkhoglyadova, O. P., Mannucci, A. J., Lakhina, G. S., Li, G., & Zank, G. P. (2009). A brief review of "solar flare effects" on the ionosphere. *Radio Science, 44*(1). https://doi.org/10.1029/2008RS004029

Wait, J. R. (1959). Diurnal change of ionospheric heights deduced from phase velocity measurements at VLF. *Proceedings of the IRE*, *47*(5), 998. http://doi.org/10.1109/JRPROC.1959.287320

Wang, Q. X, Yang, W. K., & Zhu, G. Y. (2017). Hazards of geomagnetic storms. *Life & Disaster*, (12),30-33.

Wu, Y. B. (2014). Analysis of Effect of Ionospheric Metamorphosis on Navigation Communication Satellite Communication Link. (Master's thesis). Retrieved from CNKI. (https://kns.cnki.net/kcms/detail/detail.aspx?dbcode=CMFD&dbname=CMFD201401&filename=1014177629.nh&uniplatform=NZKPT&v=m4EL-ktHt8TMyfaJwNFe37otQ-Rjr0c9BM2VNmVQVj2PmGcmIBk-ZPn3gp-ly3HF). Beijing, China: *Beijing Jiaotong University*.

Xie, L., Pu, Z. Y., Zhou, H. Z., Fu, S. Y., & Zong, Q. G. (2004). The process of magnetic storm loop current formation. *Chinese Science Bulletin, 49*(6), 603-610. http://doi.org/10.3321/j.issn:0023-074X.2004.06.019

Yi, J., Gu, X. D., Li, Z. P., Lin, R. T., Cai, Y. H., & Chen, L., et al. (2019). Modeling and analysis of NWC signal propagation amplitude based on LWPC and IRI models. *Chinese Journal of Geophysics, 62*(09), 3223-3234. http://doi.org/10.6038/cjg2019N0190

Yuan, J. P., Luo, J. J., Yue, X. K., & Fang, Q. (2003). *Satellite Navigation System: Principle and Application*. Beijing, China: China Aerospace Publishing House.

Zhang, Y. X. (2014). Research on the Application of VLF Method in Space Weather Forecasting, (Master's thesis). Retrieved from CNKI. (https://kns.cnki.net/kcms/detail/detail.aspx?FileName=1014356877.nh&DbName=CMFD2015). Xinxiang, China: Henan Normal University.

Zhou, Z. J. (2017). Research on the effect of solar flares on radio navigation system. *Engineering and Technology Research*, (04):245+251. http://doi.org/10.3969/j.issn.1671-3818.2017.04.157